Fine Structure in Electron Paramagnetic Resonance of Mn^{2+} in Zinc Sulfate*†

D. J. SUKLE AND J. S. WELLS
National Bureau of Standards, Boulder, Colorado
and
University of Colorado, Boulder, Colorado 80302
(Received 26 November 1968)

The electron spin resonance of 0.01% Mn^{2+} in single crystals of $ZnSO_4$ has been studied in order to investigate the crystal-field interaction, which may be representative of the single-ion anisotropy in $MnSO_4$. The symmetry group for the zinc site, which the Mn^{2+} ions are assumed to occupy, is C_i. There are, in general, four inequivalent zinc sites which produce a spectrum of 320 possible lines at an arbitrary orientation. However, data have been taken with H_0 in symmetry planes of the crystal so that pairs of inequivalent sites become equivalent. This results in some simplification of the spectrum and provides a method for accurate alignment of the crystal. The spectrum has been fitted to a low-symmetry spin Hamiltonian. Since crystal-field terms are large, perturbation theory could not be used, and the spin-Hamiltonian analysis of the spectrum was accomplished by computer programs that diagonalize the spin-Hamiltonian matrix. An isotropic g factor of 2.0017 ± 0.0010 and spin-Hamiltonian parameters $C_{20}=(3.792\pm0.001)\times10^{-2}$ cm^{-1}, $C_{21}=(3.815\pm0.001)\times10^{-2}$ cm^{-1}, $C_{22}=(5.808\pm0.001)\times10^{-2}$ cm^{-1} with lobe orientations $\lambda_{21}=152.6°$ and $\lambda_{22}=86.5°$ describe the room-temperature spectrum reasonably well. The inclusion of the C_{4q} terms improves the fit.

INTRODUCTION

ZINC sulfate is isomorphous with some of the anhydrous iron-group sulfates which are antiferromagnetic at helium temperatures. We have investigated $ZnSO_4$ doped with manganese as part of a program to determine the magnitude of single-ion anisotropy in $MnSO_4$, which is of current interest because of its complex magnetic structure in the antiferromagnetic state.[1,2] Figure 1 indicates the structure of the orthorhombic crystal $ZnSO_4$. The unit cell contains four equivalent but differently oriented zinc sites. Approximately 0.01% of these are occupied by Mn^{2+} ions. These sites possess only inversion symmetry; hence, a more complicated spin Hamiltonian than usual is required to describe the spectrum resulting from an electron-paramagnetic-resonance (EPR) experiment. The lack of a definite symmetry axis for the site permits one to choose an arbitrary coordinate system in which to describe the crystalline-field interaction associated with the site. The spectrum due to the Mn^{2+} ions ($S=\frac{5}{2}$, $I=\frac{5}{2}$) which occupy the four zinc sites consists of 120 first-order transitions, and may be further complicated by the presence of over 200 "forbidden transitions." The experimentally observed spectrum simplifies for certain restrictions (related to the crystal symmetry) on the magnetic field direction. This simplification dictates the choice of a coordinate system for the analysis of the spectrum. The magnitude of the parameters in the spin Hamiltonian precluded the use of perturbation theory, hence direct diagonalization was required to analyze the data. Diagonalization and parameter fitting were accomplished with the aid of computer techniques.

EXPERIMENTAL

The experimental investigation was conducted in a K-band spectrometer operating at 23.3 GHz. An automatic frequency-control (AFC) circuit locked the klystron to the frequency of the spiral-groove sample

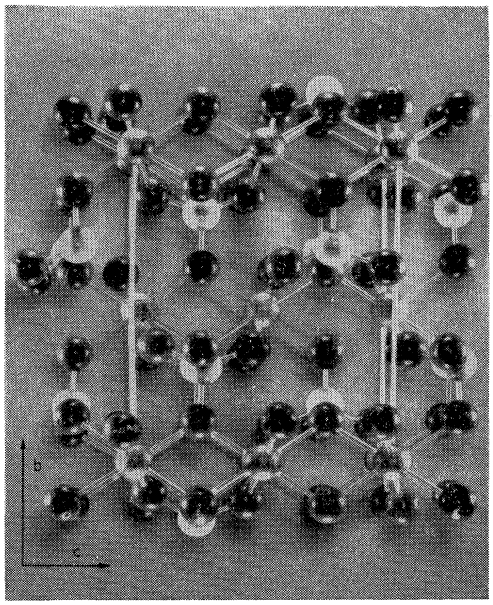

FIG. 1. Photograph of a model of $ZnSO_4$. The light-colored spheres represent sulfur atoms. The dark spheres representing oxygen atoms form distorted octahedra about the shaded spheres which represent zinc ions. The Mn^{2+} ions go into the lattice substitutionally for the zinc. We use the notation where the lattice constants are $a=4.77$ Å, $b=8.58$ Å, and $c=6.73$ Å. The b and c axes are indicated in the figure.

* Research supported in part by the National Science Foundation.
† Work based on a portion of D. J. Sukle's Ph.D. thesis at the University of Colorado.
[1] G. Will, B. C. Frazer, G. Shirane, D. E. Cox, and P. J. Brown, Phys. Rev. **140**, A2139 (1965).
[2] Y. Allain, J. P. Krebs, and J. de Gunzbourg, J. Appl. Phys. **39**, 1124 (1968).

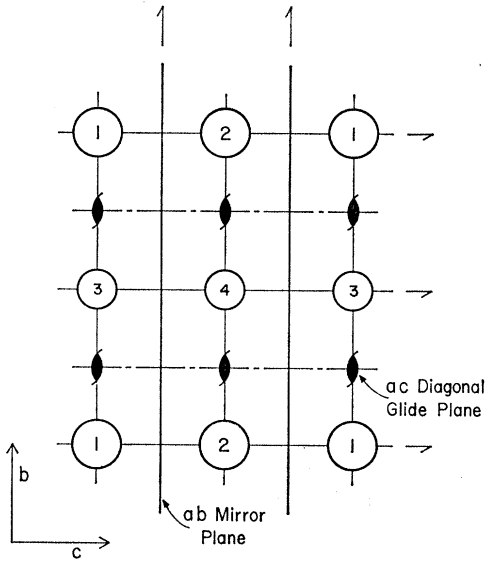

FIG. 2. Sketch representing a unit cell shows the location of four inequivalent zinc ions and the pertinent symmetry operations. The sulfur and oxygen positions are omitted for clarity. Sites 3 and 4 are positioned in a *bc* plane located $\frac{1}{2}a$ from the *bc* plane containing sites 1 and 2. The relevant symmetry operations include the *ab* mirror plane *m*, three orthogonal twofold screw axes, and two glide planes. The *ac* diagonal glide plane carries site 1–4 and 3–2. The *bc* glide planes located at $\frac{1}{4}a$ and $\frac{3}{4}a$ transform site 1–3 and site 2–4.

cavity.[3] Frequencies were measured by a cavity wavemeter which was calibrated by National Bureau of Standards (NBS). Magnetic field modulation of 100 kHz and the usual phase-sensitive detection techniques were used to display the derivative of the absorption on an *X-Y* plotter. The *X* axis was driven by a transmitter in the field control system, which used a Hall device to measure the field in the 15-in. magnet. A nuclear resonance fluxmeter and frequency counter were used to obtain precise field measurements.

The $ZnSO_4$ crystals which contain about 0.01% Mn^{2+} were grown by Gruzensky at NBS Boulder Labs. X-ray and optical techniques were used to orient the crystals. The Mn^{2+} ions are assumed to occupy the sites of the diamagnetic zinc ions. The structure of $ZnSO_4$ has been determined by Kokorros and Rentzeperis[4] and belongs to the space group Pbnm. The zinc sites and some of the relevant symmetry operations are indicated in Fig. 2. Sites labeled 1, 2, 3, and 4 are magnetically inequivalent in the sense that their crystal environments are related by mirror or glide reflections rather than by simple translations. For arbitrary orientations of H_0, four inequivalent EPR spectra are thus observed; however, when H_0 is parallel to a mirror or glide plane relating two inequivalent sites, these sites then have equivalent spectra. There is a symmetry plane parallel to each of the crystal planes *ab*, *bc*, and *ca*, and each symmetry plane relates two pairs of sites. When H_0 is parallel to the crystal axes *a*, *b*, or *c*, all sites become equivalent.

These considerations allow one to accurately align the crystal. A specially designed sample orientation servo[5] was constructed in order to utilize these symmetry aids in positioning the sample. This servo permits one to change the orientation of the crystal by an external manipulator and to observe subsequent changes in the spectrum without removing the crystal from the spectrometer and thus use an iterative procedure to align the crystal.

The complicated spectrum simplifies upon desired alignment. The spectrum has been recorded at 5° intervals with H_0 in the *ab*, *bc*, and *ca* planes of the crystal unit cell. Angular variation in this "simplified spectrum" with H_0 parallel to the *ab* plane is shown in Fig. 3(a). The "allowed" lines are grouped in sets of six corresponding to the $\Delta M = \pm 1$ transitions between the states $|M,m\rangle$ and $|M\pm1, m\rangle$, where M and m are, respectively, the electron and nuclear magnetic quantum numbers. The (usually) weaker lines situated

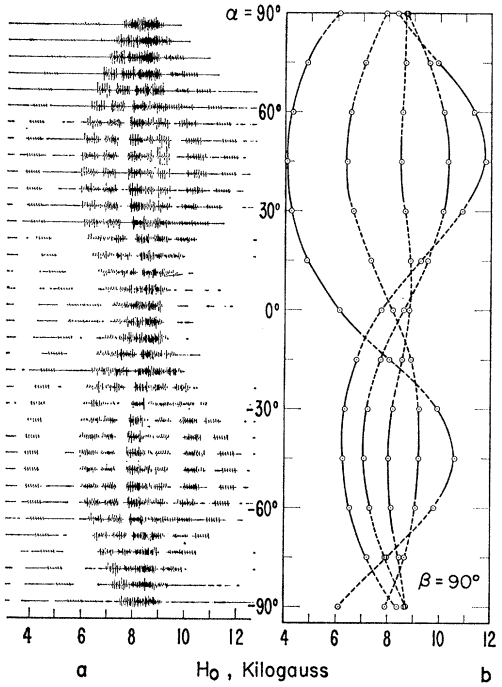

FIG. 3. (a) Experimental traces indicating angular variation in the EPR spectrum of Mn^{2+} in $ZnSO_4$, with H_0 in the *ab* plane. The magnetic field ranges from 4 to 12 kG. Successive traces are taken at 5° intervals from $\alpha = -90°$ to $+90°$. Zero degrees corresponds to H_0 parallel to the *a* axis of the crystal. (b) indicates the center of the hyperfine set from one site. The dashed portions indicate regions where it was difficult to make accurate determinations of the set centers. The points inside the circles represent computer-generated points based on the spin-Hamiltonian parameters indicated in Table I.

[3] A. R. Cook, L. M. Matarrese, and J. S. Wells, Rev. Sci. Instr. **35**, 114 (1964).

[4] P. A. Kokkoros and P. J. Rentzeperis, Acta Cryst. **11**, 361 (1958).

[5] D. J. Sukle and J. S. Wells, Rev. Sci. Instr. **39**, 604 (1968).

outside and between these lines appear to be transitions of the type $\Delta M=\pm 1$, $\Delta m=\pm 1$. These have been investigated by Bleaney and Rubins[6] and Drumheller and Rubins[7] and have been shown to be due to mixing of states by cross terms resulting from off-diagonal parts of the crystalline-field interaction and the hyperfine interaction $AI\cdot S$. The locations of these lines with respect to the allowed lines are characteristic of the value M in the transition $M\rightarrow M+1$, and thus serve as an additional aid in identifying the transitions. The angular variation is shown more clearly in Fig. 3(b), where only the centers of the hyperfine group from one site are indicated.

Theory

The ground state of the free Mn^{++} ion is ${}^6S_{5/2}$. In the combined crystal field and external magnetic field, six low-lying electron spin states are observed in the EPR experiment. The nuclear spin of Mn is $I=\frac{5}{2}$, so that the hyperfine interaction causes a sixfold splitting of each electron spin state. First-order magnetic dipole selection rules are $\Delta M=\pm 1$, $\Delta m=0$. Thus, when states can be labeled by the quantum numbers M and m, we may observe 30 allowed magnetic dipole transitions in the Mn^{2+} ion. In general, the states are mixed so that "forbidden" $\Delta m=\pm 1$ (and in some cases $\Delta M=\pm 2$) transitions may be observed.

The spin Hamiltonian for a Mn^{2+} ion in a crystal environment and an external magnetic field has the general form

$$\mathcal{H}=\beta\mathbf{H}\cdot\mathbf{G}\cdot\mathbf{S}+\mathbf{I}\cdot\mathbf{A}\cdot\mathbf{S}+\mathcal{H}_{cr}+\mathcal{H}_{qn}, \tag{1}$$

where β is the Bohr magneton, H is the external field, $\mathbf{G}$ is the g tensor, $\mathbf{A}$ is the hyperfine interaction tensor, I and S are the nuclear and electron spin operators, and $\mathcal{H}_{cr}$ represents the crystalline-field interaction. $\mathcal{H}_{qn}$ includes possible quadrupole and nuclear interactions which would be masked by the large $\mathcal{H}_{cr}$ term for this experiment. The $\mathcal{H}_{cr}$ term gives rise to the angular variation referred to as fine structure of the spectrum. Since the fine-structure interaction is large, we may regard the hyperfine interaction as a perturbation and consider it in first order but neglect its small second-order corrections in interpreting the spectrum. We thus consider the zero-order spin Hamiltonian

$$\mathcal{H}_0=\beta\mathbf{H}\cdot\mathbf{G}\cdot\mathbf{S}+\mathcal{H}_{cr}. \tag{2}$$

The angular variation depends on the symmetry of the location of electric charges, shown in Fig. 4, which constitute the environment of the magnetic ion. It is convenient[8] to express the matrix for $\mathcal{H}_{cr}$ in terms of the standard components of the irreducible spin-tensor

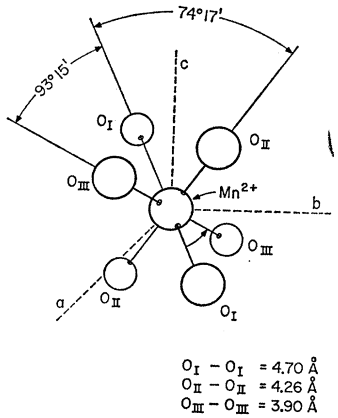

FIG. 4. Sketch of Mn^{2+} and the surrounding oxygens indicating distortion from regular octahedron. Distances between ions and angles between lines joining ions are indicated on sketch. Data are taken from Kokkoros and Rentzeperis.

operator $T_q^{(k)}$. Here k is a positive integer and q is any integer such that $|q|\leqslant k$. The $T_q^{(k)}$'s may be defined by specifying their commutation relations with the spin operators S_z, $S_\pm$:

$$[S_\pm,T_q^{(k)}]=[k(k+1)-q(q\pm 1)]^{1/2}T_{q\pm 1}^{(k)},$$
$$[S_z,T_q^{(k)}]=qT_q^{(k)}. \tag{3}$$

As a result of these relations, the $T_q^{(k)}$'s transform according to the $D^{(k)}$ representation of the full rotation groups; that is, they transform like spherical harmonics. Their matrix elements in the representation $|SM\rangle$ are given in terms of the Clebsch-Gordan coefficients $\langle SM'kq|SM\rangle$ by the Wigner-Eckart formula

$$\langle SM|T_q^{(k)}|SM'\rangle = (2S+1)^{-1/2}\langle S\|T_q^{(k)}\|S\rangle\langle SM'kq|MS\rangle. \tag{4}$$

The quantity $\langle S\|T_q^{(k)}\|S\rangle$, called the reduced matrix element, depends only on k and S. The Hermitian conjugate may be defined as

$$\langle SM|T_q^{(k)}|SM'\rangle^\dagger=\langle SM'|(-1)^qT_{-q}^{(k)}|SM\rangle. \tag{5}$$

The crystal-field part of the spin Hamiltonian may be written as the linear combination

$$\mathcal{H}_{cr}=\sum_{k=0}^{5}\sum_{q=-k}^{k}A_q^kT_q^{(k)}; \tag{6}$$

$T_q^{(k)}$'s with $k>5$ cannot contribute because the Clebsch-Gordan coefficient of Eq. (4) is zero for $k>2S=5$. We may discard the $k=0$ term, since this shifts all levels by the same amount. Also, the spin Hamiltonian should be invariant with respect to time reversal (applied to the external field source as well as the crystal system). This requires coefficients for odd k to be zero since $T_q^{(k)}$'s with k odd change sign under time reversal. Additional terms cannot be discarded by symmetry arguments, since the Zn site is invariant only with respect to inversion, which eliminates the same

[6] B. Bleaney and R. S. Rubins, Proc. Phys. Soc. (London) 77, 103 (1961).
[7] J. E. Drumheller and R. S. Rubins, Phys. Rev. 133, A1099 (1964).
[8] C. Kikuchi and L. M. Matarrese, J. Chem. Phys. 33, 601 (1960).

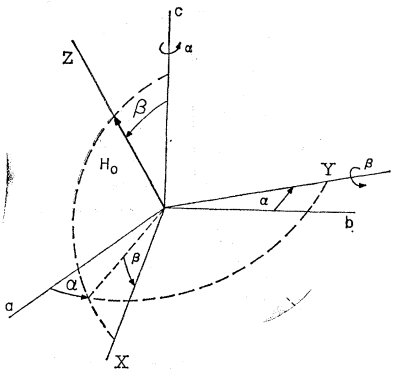

FIG. 5. Sketch showing angles relating the crystal coordinate system a, b, and c to the field specified system X, Y, and Z. The angle γ in the rotation matrix [Eq. (10)] is zero.

terms as time-reversal considerations. We require the spin Hamiltonian to be Hermitian, so

$$A_q{}^k=(-1)^q A_{-q}{}^{k*}. \tag{7}$$

We write the constants $A_q{}^k$ as an amplitude C_{kq} and a phase factor $e^{i\lambda_{kq}}$, where the λ_{kq} corresponds to a lobe orientation.[9] We finally write

$$\begin{aligned}\mathcal{H}_{cr}=&C_{20}T_0{}^{(2)}+C_{21}(T_1{}^{(2)}e^{-2i\lambda_{21}}+T_{-1}{}^{(2)}e^{+2i\lambda_{21}})\\&+C_{22}(T_2{}^{(2)}e^{-2i\lambda_{22}}+T_{-2}{}^{(2)}e^{2i\lambda_{22}})+C_{40}T_0{}^{(4)}\\&+C_{41}(T_1{}^{(4)}e^{-2i\lambda_{41}}+T_{-1}{}^{4}e^{2i\lambda_{41}})\\&+C_{42}(T_2{}^{(4)}E^{-2i\lambda_{42}}+T_{-2}{}^{(4)}e^{2i\lambda_{42}})\\&+C_{43}(T_3{}^{(4)}e^{-2i\lambda_{43}}+T_{-3}{}^{4}e^{2i\lambda_{42}})\\&+C_{44}(T_4{}^{(4)}e^{-2i\lambda_{44}}+T_{-4}{}^{(4)}e^{2i\lambda_{44}}),\end{aligned} \tag{8}$$

where to exhibit the normalization, we write the $T_q{}^{(k)}$ explicitly in terms of S_z, S_+, and S_-:

$$\begin{aligned}T_0{}^{(2)}&=S_z{}^2-\tfrac{1}{3}S(S+1),\\T_{\pm1}{}^{(2)}&=(1/\sqrt{6})(S_zS_\pm+S_\pm S_z),\\T_{\pm2}{}^{(2)}&=(1/\sqrt{6})S_\pm{}^2,\\T_0{}^{(4)}&=\tfrac{1}{8}[35S_z{}^4-30S(S+1)S_z{}^2+25S_z{}^2\\&\qquad+3S^2(S+1)^2-6S(S+1)],\\T_{\pm1}{}^{(4)}&=(\sqrt{5}/8)S_\pm(2S_z\pm1),\\T_{\pm2}{}^{(4)}&+(\sqrt{10}/8)S_\pm{}^2[S(S+1)-9\mp14S_z-7S_z{}^2],\\T_{\pm3}{}^{(4)}&=(\sqrt{35}/8)S_\pm{}^3(2S_z\pm3)\\T_{\pm4}{}^{(4)}&=(\sqrt{70}/16)S_\pm{}^4.\end{aligned} \tag{9}$$

We have obtained $\mathcal{H}_{cr}$ without appealing to any symmetry arguments which depend on a particular coordinate system (e.g., we have not discarded any terms because of the presence of an n-fold rotational-symmetry axis); thus, (8) is valid in any coordinate system. Since it is most convenient to obtain data in the symmetry planes of the crystal, we shall take the axes of quantization for Eq. (8) to be the unit cell axes of the crystal. It is convenient to express (2) in the coordinate system for which the Zeeman term is diagonal; that is, in the system XYZ, where Z is parallel to $\mathbf{H}_0$. Both $\mathbf{H}_0$ and $\mathbf{S}$ transform as vectors so that the Zeeman term becomes $g\beta H_0S_z$ in the new system as g was observed to be isotropic. The transformation of the $T_q{}^{(k)}$'s is given by

$$T_q{}^{(k)}=\sum_{q'}R_{qq'}{}^{k*}(\alpha,\beta,\gamma)T_{q'}{}^{(k)}, \tag{10}$$

where the $T_q{}^{(k)}$'s in the summation are referred to the new coordinate system. The transformation coefficients are

$$R_{qq'}(\alpha\beta\gamma)=\langle S,q'|\,e^{-i\alpha J_z}e^{-iJ_y\beta}e^{-iJ_z\gamma}\,|S,q\rangle. \tag{11}$$

The angles α, β, γ are the Euler angles for the transformation taken in the convention of Messiah. With this convention, α and β are the azimuthal and polar angles, respectively, of H_0 with respect to the crystal axes, as indicated in Fig. 5. Substituting Eq. (10) into (8), we obtain the spin Hamiltonian in the system, X, Y, Z:

$$\mathcal{H}=\sum_{k=2,4}\sum_{q=-k}^{k}K_q{}^kT_q{}^k+g\beta H_0S_z, \tag{12}$$

where

$$K_{\pm|q|}{}^k=\sum R_{qq}{}^{(k)*}(\alpha\beta\gamma)(\pm1)^qe^{\pm i\lambda_{kq}}C_{kq}. \tag{13}$$

Results

The process of fitting the data to the $\mathcal{H}_{cr}$ of (8) is complicated by several difficulties. The absence of any special symmetry axis precludes the possibility of taking measurements along directions for which only one term (say the axial or rhombic) contributes. Also related to the low symmetry of the site is the large number of terms to be considered in the spin Hamiltonian. Finally, the large observed fine-structure splitting suggests that perturbation theory is not valid, at least for most orientations of H_0. We have thus accomplished the fitting to the spin Hamiltonian using computer techniques.

It is a straightforward matter to generate the transformation coefficients $R_{qq'}{}^{(k)}(\alpha,\beta,\gamma)$ from the formula

$$R_{MM'}{}^{(J)}=e^{-i\alpha M}\mathcal{R}_{MM'}{}^{(J)}e^{-i\gamma M'}, \tag{14}$$

where $\mathcal{R}_{MM'}{}^{(J)}$ is given by the Wigner formula

$$\begin{aligned}\mathcal{R}_{MM'}{}^{(J)}&=\sum_t(-1)^t\frac{((J+M)!(J-M)!(J+M')!(J-M')!)^{1/2}}{(J+M-t)!(J-M'-t)!t!(t-M+M')!}\\&\quad\times(\cos\tfrac{1}{2}\beta)^{2J+M-M'-2t}(\sin\tfrac{1}{2}\beta)^{2t-M+M'}.\end{aligned} \tag{15}$$

The summation is for all t for which the arguments of the factorials are zero or positive. Having generated the R's, the coefficients $K_q{}^k$ in the rotated system may be calculated. The matrices of the $T_q{}^{(k)}$'s are easily

[9] R. L. Peterson, L. M. Matarrese, and J. S. Wells, Natl. Bur. Std. (U. S.) Tech. Note 372 (1968).

TABLE I. Spin-Hamiltonian parameters.

$g=2.0017$	
$C_{20}=3.7921\times10^{-2}$ cm^{-1}	
$C_{21}=3.8153\times10^{-2}$ cm^{-1},	$\lambda_{21}=152.6°$
$C_{22}=5.8077\times10^{-2}$ cm^{-1},	$\lambda_{22}=86.5°$
$C_{40}=1.954\times10^{-5}$ cm^{-1}	
$C_{41}=2.874\times10^{-5}$ cm^{-1},	$\lambda_{41}=53.3°$
$C_{42}=8.066\times10^{-5}$ cm^{-1},	$\lambda_{42}=54.9°$
$C_{43}=-3.406\times10^{-5}$ cm^{-1},	$\lambda_{43}=-25.6°$
$C_{44}=3.231\times10^{-5}$ cm^{-1},	$\lambda_{43}=62.3°$

generated from the Wigner-Eckart formula (4), so the matrix of the spin Hamiltonian in the rotated system may be generated. This can then be diagonalized by the computer. The eigenvalues depend on the value of the spin-Hamiltonian parameters, plus the magnitude and orientation of the external field.

A more difficult problem is to search for the proper parameters in a systematic way. We have employed the subroutine VA02A written by Powell. This is an efficient searching routine[10] that finds a set of N parameters X_i which minimizes the function

$$F=\sum_{i=1}^{M}[F_i(X_i\cdots X_M)]^2, \tag{16}$$

where the M functions F_i depend on the parameters X_i. No analytical expression need be provided for the F_i's, but the programmer must provide a subroutine which generates the M values F_i given a set of parameters X_i. In the iterative searching process, VA02A transmits sets of parameters X_i to this subroutine and receives the values of F_i. The search is terminated when certain accuracy criteria are satisfied. We take the parameters X_i to be the spin-Hamiltonian parameters and let the functions F_i be the values $E_M(\alpha,\beta,H)-E_{M-1}(\alpha,\beta,H)-h\nu$, where $E_M(\alpha,\beta,H)$ and $E_{M-1}(\alpha,\beta,H)$ are the eigenvalues of the states M and $M-1$ obtained by diagonalization of the spin-Hamiltonian matrix. The value of H_0 is taken as the observed resonance field for the transition $M-1\rightarrow M$ and ν is the resonant frequency of the sample cavity.

Unfortunately, VA02A (and similar fitting programs) tend to converge upon the nearest local minimum, rather than the absolute minimum, so it is necessary to provide a reasonable initial estimate for the spin-Hamiltonian parameters. A satisfactory initial estimate was obtained with the aid of a second program, similar to the one above, which searches for resonance fields given a set of spin-Hamiltonian parameters. The fields are plotted as a function of orientation on the standard output unit of the computer. We were then able to pick a set of parameters which yielded an angular variation of the line positions with the same gross features as the experimental spectrum. These parameters were used as a starting point for the fitting program.

TABLE II. Experimental and calculated resonance fields in kG.

Angles α,β		Transition $\frac{5}{2}$	$\frac{3}{2}$	$\frac{1}{2}$	$-\frac{1}{2}$	$-\frac{3}{2}$
0°, 0°	Expt	6.489	7.349	8.233	9.086	9.498
	Calc	6.492	7.347	8.234	9.070	9.501
0°, 25°	Expt	5.868	6.929	8.070	9.354	10.945
	Calc	5.863	9.930	8.055	9.350	10.943
90°, 20°	Expt	6.545	7.189	7.998	9.003	10.255
	Calc	6.545	7.194	7.999	9.005	10.268
45°, 90°	Expt	11.729	10.310	8.486	6.369	4.078
	Calc	11.728	10.308	8.487	6.371	4.080
−45°, 90°	Expt	6.233	7.067	8.026	9.167	10.587
	Calc	6.233	7.068	8.027	9.169	10.582

[10] M. J. D. Powell, Computer J. 7, 155 (1964).

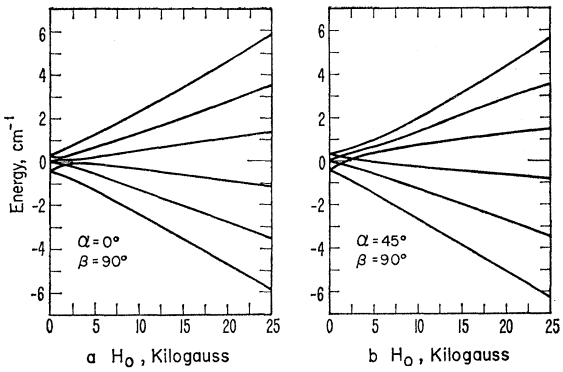

FIG. 6. Energy levels as a function of field for Mn^{2+} in $ZnSO_4$ are shown for two orientations of the magnetic field. Mixing of levels at lower fields is indicated by a large amount of "level repelling." (a) corresponds to H_0 along the crystal axis a and indicates the reason the spectrum is crowded at this orientation. (b) corresponds to a very large separation between transitions.

The final set of parameters produced by the fitting program was inserted into the computer along with another program which determined and plotted line positions. A reasonably good agreement between computer generated points and experimental data was obtained using only C_{2q} terms. A better fit was obtained by including the C_{4q} terms. The points indicated in Fig. 3(a) included both C_{2q} and C_{4q} terms.

The spin-Hamiltonian parameters used to obtain this fitting are listed in Table I.

Table II indicates the degree to which these parameters describe the spectrum. The line positions were obtained using both C_{4q} and C_{2q} terms. The average magnitude of deviation is about 4 G. When only C_{2q} terms were used this average deviation increased to about 6 G; hence, for practical purposes the C_{2q} terms describe the spectrum.

A study of the hyperfine interaction has been deferred to a later date. Such an investigation would more profitably be done at a higher field, say 25 kG where the mixing of levels and the intensity of the forbidden lines would be smaller. Also, one could use perturbation theory and obtain explicit expressions for forbidden-line intensities. As may be seen from Fig. 6, the high-field region involves "relatively pure" states as compared to the region where this experiment was performed.

In summary, the crystalline-field interaction of Mn^{2+} in $ZnSO_4$ has been investigated and reasonably good numbers obtained to characterize it. It is anticipated that these results along with other information may be useful in the elucidation of the complex structure of $MnSO_4$. The role that single-ion anisotropy would play in an antiferromagnetic resonance experiment[11] in a structure as complex as $MnSO_4$ has yet to be determined; however, this work along with a dipolar field calculation should be useful in estimating a lower bound for the zero-field energy gap.

[11] G. F. Herrmann, J. Phys. Chem. Solids 24, 497 (1963).

ACKNOWLEDGMENTS

We would like to thank Dr. P. Gruzensky for growing the crystals used in this experiment. We are also grateful not only for helpful discussions with and support from Professor W. H. Tanttila, but also for the use of his facilities during preliminary phases of the work. Discussions with Professor R. N. Rogers regarding fitting programs are also greatly appreciated.

PHYSICAL REVIEW VOLUME 180, NUMBER 2 10 APRIL 1969

Small-Angle Scattering of S^{32} and O^{16} Beams in Thin Foils*

C. K. Cline, T. E. Pierce, K. H. Purser, and M. Blann
Nuclear Structure Research Laboratory, University of Rochester, Rochester, New York 14627
(Received 17 October 1968)

The rms scattering angles introduced into beams of 10- to 70-MeV O^{16} ions and 10- to 110-MeV S^{32} ions by passage through thin foils of carbon, beryllium oxide, and aluminum oxide have been measured. The foils used ranged in thickness from 5 to 50 $\mu g/cm^2$. Qualitative agreement with the predictions of multiple Coulomb scattering theory is found, but an over-all normalization factor of 1.8 was needed in most cases to obtain quantitative agreement with the data.

I. INTRODUCTION

WHEN an ion beam passes through a foil, multiple electronic interactions occur which cause energy spreads and small-angle scattering to be introduced. With light particle beams, these effects are usually ignored, but with heavy ions they can become experimentally significant. A knowledge of the magnitude of the dispersions introduced into heavy ion beams by foils is, therefore, important in at least two applications. The first is in the design of proposed heavy-ion accelerators, which utilize foil strippers to increase the charge on the beam particles. A knowledge of the angular spread of the beam is important in determining the transmission efficiencies of such accelerators. Secondly, a knowledge of the magnitude of the angular spread is essential for estimating the loss of resolution in experiments which involve the detection of heavy-ion-beam particles after passage through a target foil.

Previous work investigating the small-angle scattering of heavy ions in thin foils has been carried out by Hortig and Rogge,[1] using beams of fluorine, arsenic, and iodine ions in foils of carbon, aluminum, and gold. The beam energies used range from 8 to 75 MeV. The work presented here was designed to measure the magnitude of small-angle scattering with other beams and other targets. This effect has been measured as a function of beam energy, beam particle, target material, and target thickness.

II. EXPERIMENTAL PROCEDURE

The experimental apparatus is shown in Fig. 1. A beam of heavy ions accelerated by the University of Rochester MP Tandem Van de Graaff accelerator was collimated by passage without focusing through two sets of 1×1.5-mm defining slits placed 8 m apart. The beam was then allowed to pass through a scattering foil and was stopped in a CsI scintillator which was optically coupled to the inside of a glass viewing plate. The light produced by the beam particles incident on the crystal could then be observed directly. The cesium iodide crystal was at a known distance (158 cm) from the scatterer so that measured beam diameters could be converted into mean scattering angles.

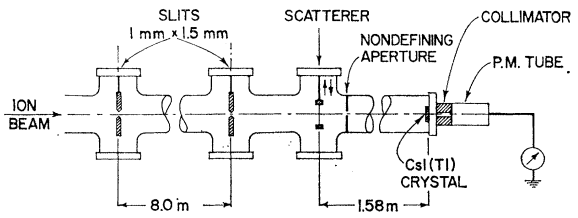

FIG. 1. Diagram of the apparatus used for measuring beam diameters.

* This work was supported by the U. S. Atomic Energy Commission and the U. S. Air Force Office of Scientific Research.

[1] G. Hortig and M. Rogge, Annual Report, Max-Planck Institute, Heidelberg, 1966 (unpublished).

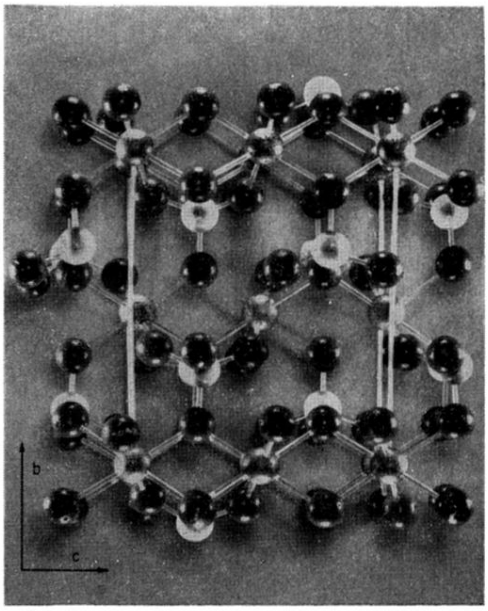

FIG. 1. Photograph of a model of $ZnSO_4$. The light-colored spheres represent sulfur atoms. The dark spheres representing oxygen atoms form distorted octahedra about the shaded spheres which represent zinc ions. The Mn^{2+} ions go into the lattice substitutionally for the zinc. We use the notation where the lattice constants are $a=4.77$ Å, $b=8.58$ Å, and $c=6.73$ Å. The b and c axes are indicated in the figure.